

Radiation Patterns of Three Element SteppIR Antennas: Measurements and Computer Models.

Georg Efremidis, DJ3AA, Helmut Hengstenberg, DL9CI, und Rolf Schick, DL3AO

Introduction.

Horizontal radiation patterns of three element steppIR Yagi antennas at the stations of DJ3AA (fig.1) and DL9CI (fig.2) were measured at the recording site of DL3AO (fig.3). The distances between transmitter and receiver are 10.4 km, resp. 6.2 km. The terrain profiles are presented in figs. 4-5 . There are no larger diffraction points included in the paths and the terrain around the stations is free from hills causing possible diffusive side reflections. The measurements were made on the bands from 14 MHz to 28 MHz with the steppIR antenna settings “normal mode”, “reverse mode” and “bidirectional mode”. The following report, however confines to the measurements and interpretations made on 18 MHz in the setting “normal mode”. The measured patterns are compared and discussed with computer models.



Fig. 1: SteppIR Yagi at DJ3AA



Fig. 2 : SteppIR Yagi at DL9CI

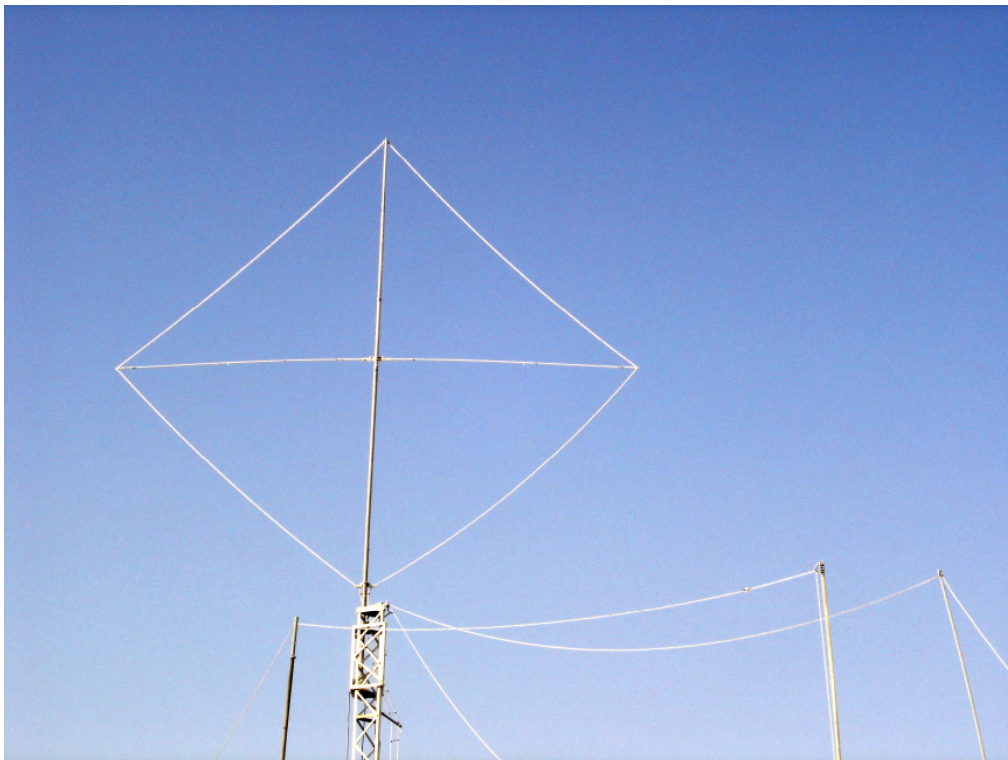


Fig. 3 : Quadloop at DL3AO

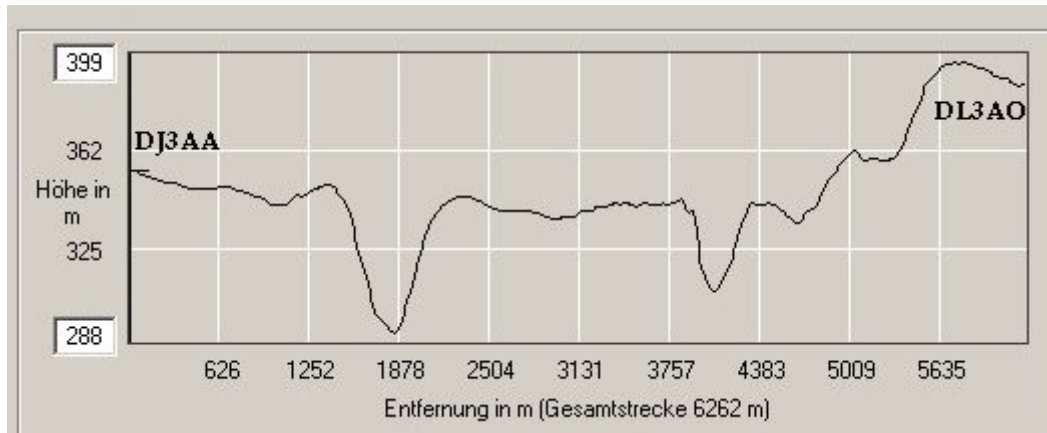


Fig. 4: Terrain profile DJ3AA – DL3AO, Bearing to DL3AO 187 deg.

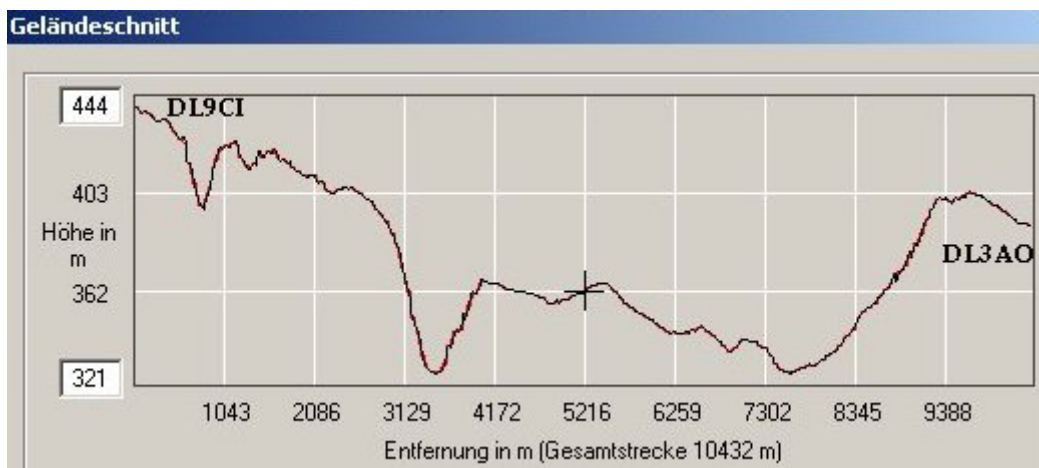


Fig. 5: Terrain Profile DL9CI – DL3AO, Bearing to DL3AO 146 deg.

Methods of Measurement.

The antenna at the recording site of DL3AO is a horizontally polarized quadloop (fig. 3). The measurement of the signal strength was carried out with a Kenwood transceiver, model TS850. The ACC2 connector on the rear side of the transceiver gives from pin 6 to pin 8 (Ground) an output voltage related to the S-meter (AVC) voltage. With the help of a RF Noise Generator (Type Hirschmann, UPR60) and a precision RF Attenuator (Wandel und Goltermann Co, fig. 6) differences in decibels between the antenna input signal at the TS850 and the output voltage at the ACC2 connector were measured with a digital meter. The obtained calibration curve is given in fig. 7.

Full scale on the S-Meter (s9+60 dB) produces an S-Meter voltage of 5 V. Zero dB on the calibration scale of fig. 7 corresponds to about 1 MikroVolt antenna input voltage. The power level with the transmitting stations was between 50 – 100 W. This was sufficient to obtain for all measurements a signal-to noise ratio exceeding 20 dB. A power and SWR meter in the antenna cable checked the constancy of the power output during the rotation of the antenna. Signal recordings were performed in 10 degree steps, rotating the antenna 360 degrees. In the “normal mode” operation of the antenna the main lobe beams to north with a rotator position of 0 or 360 degree.

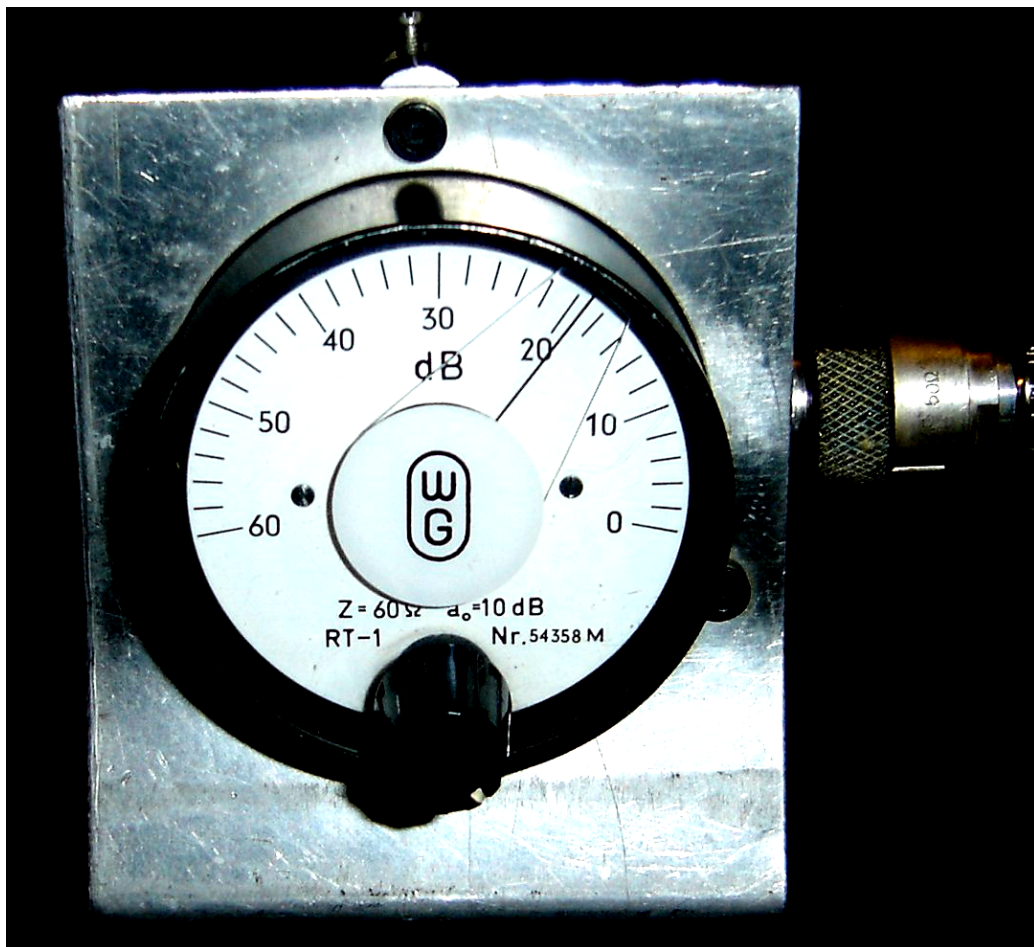


Fig. 6: Precision Attenuator (Wandel und Goltermann Co. , Germany). Measuring range 60 dB, resolution 1 dB.

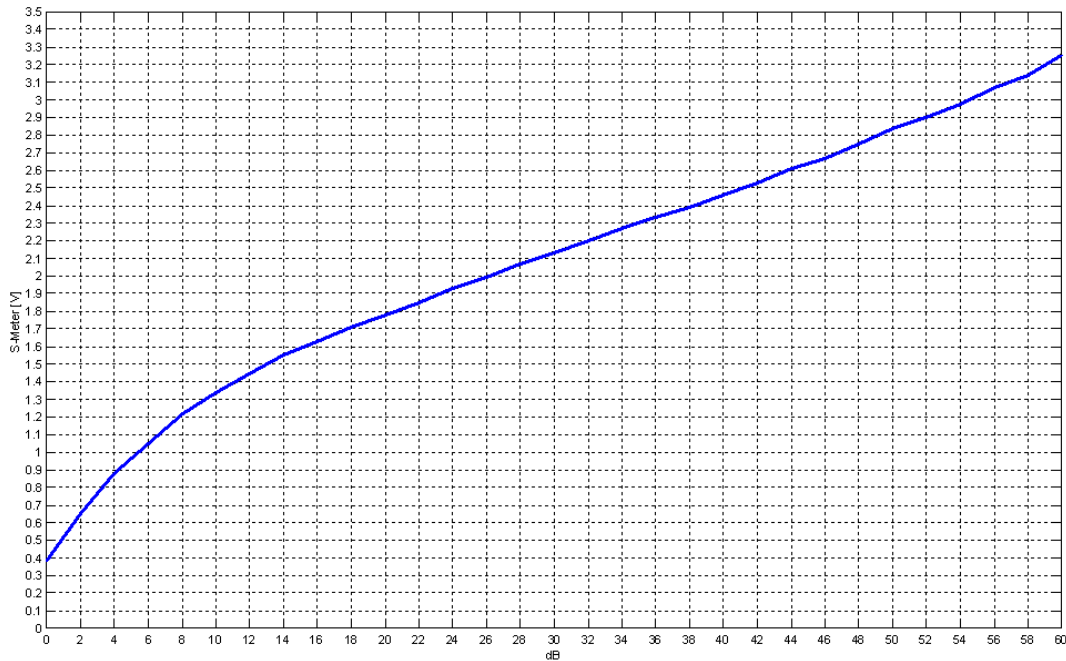


Fig. 7: S-meter voltage at ACC2 connector of TS850 [V] versus the difference in input voltage coming from the noise generator at the antenna connector TS850 in [dB].

Results.

Figs. 8a,b and figs. 9a,b depict measured radiation patterns in cartesian coordinates for the antennas with DJ3AA and DL9CI. The measurements were made following the antenna element dimensions calibration given by steppIR as “factory default (preset) element lengths”, for 18.1 MHz and for “normal mode” operation (Tab. 1).

The recorded signal strengths in these and in following figures are given both in a decibel (figs. 8a,b) and in a power scale (figs. 9a,b). The logarithmic decibel scale is advantageous for determining front-to-rear ratios. The linear power scale is favourable for determining the half-power bandwidth. The diagrams with the decibel scale show polygons connecting the measuring points. With the power scales, the curves are polynomials fitted to the data. The polynomials permit a higher accuracy with the determination of the power bandwidth (in the figs. named “Oeffnungswinkel”)

SteppIR 18 MHz normal	Director	Driven Element	Reflector
Element lengths (inch)	287.2	302.2	318.4
Element lengths (Meter)	7.29	7.67	8.04

Tab. 1: steppIR element lengths for 18 MHz, default setting, normal mode.

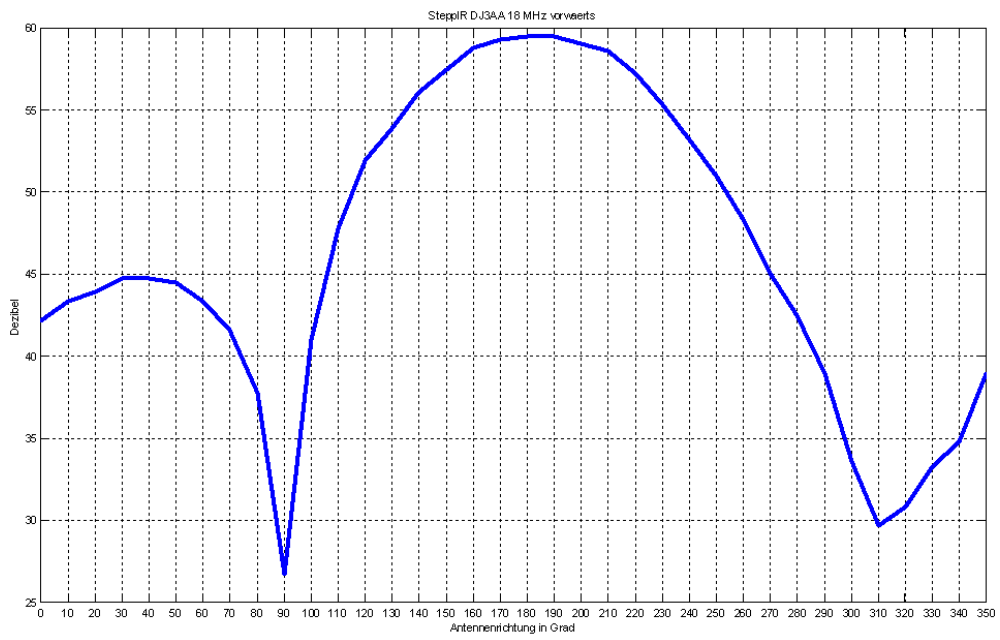


Fig. 8a: Radiation Pattern, decibel scale, 18 MHz, Normal Mode, DJ3AA

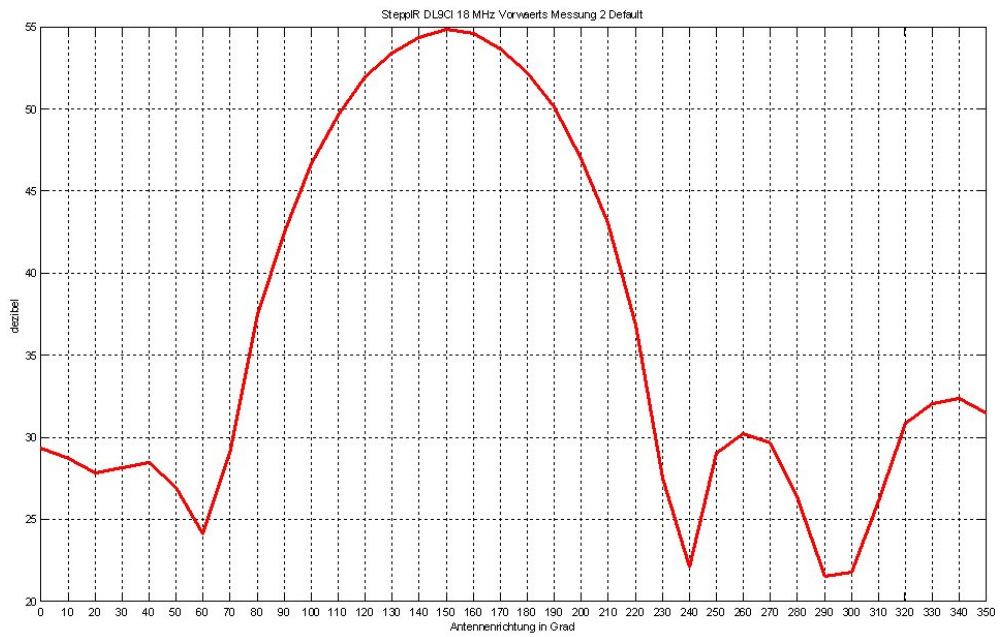


Fig. 8b: Radiation Pattern, decibel scale, 18 MHz, Normal Mode, DL9CI

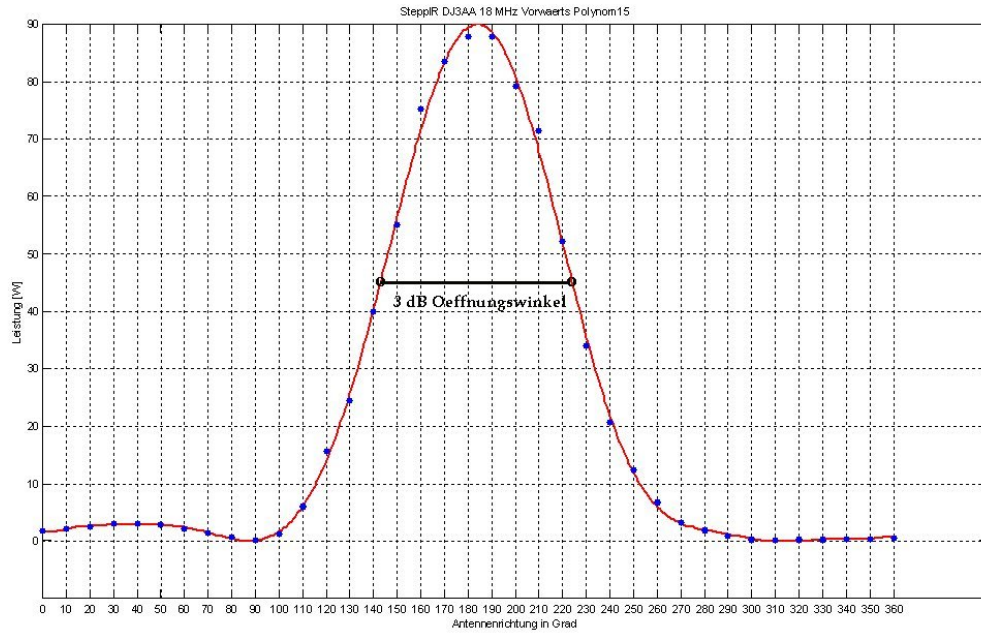


Fig. 9a: Radiation Pattern, power scale, 18 MHz, Normal Mode, DJ3AA

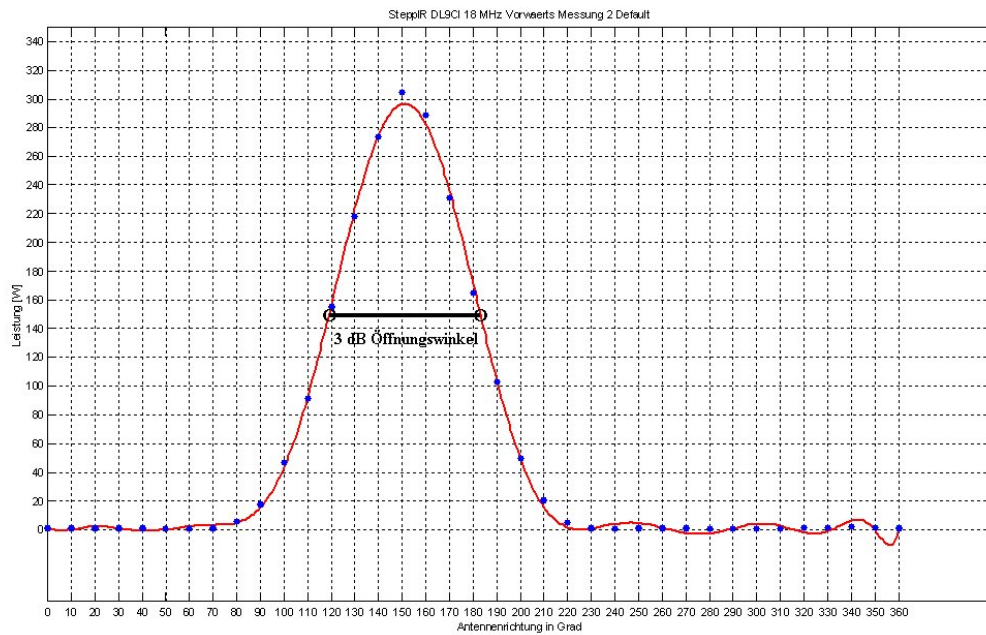


Fig. 9b: Radiation Pattern, power scale, 18 MHz, Normal Mode, DL9CI

Discussion

SteppIR specifies four quantities concerning the radiation of the antenna:

- (1) Standing Wave Ratio (SWR), relating to 50 Ohms at the feed point
- (2) Front to Back Ratio (F/B): Maximum of main lobe to maximum back lobe (180 degrees rear side).
- (3) Front to Rear Ratio (F/R): Maximum of main lobe to maximum of both back lobes and side lobes, rear side
- (4) Gain of antenna versus dipole [dBd] in free space.

The SWR with the described and in figs. 8,9 illustrated measurements showed a SWR of 1.1 or better, including a small change in SWR with antenna rotation. A clear resonance point around 18.1 MHz was found. Performing a computer simulation with EZNEC and using the element dimensions as given in Tab. 1 together with the element spacing for “normal mode”, one obtains fig. 10. The SWR curve in fig. 10 refers to a feed- point impedance of 22 Ohms. SteppIR uses a balun-unun coupler for transforming the symmetrical input impedance of the driven element to an unsymmetrical 50 Ohms for the connection of the coax cable.

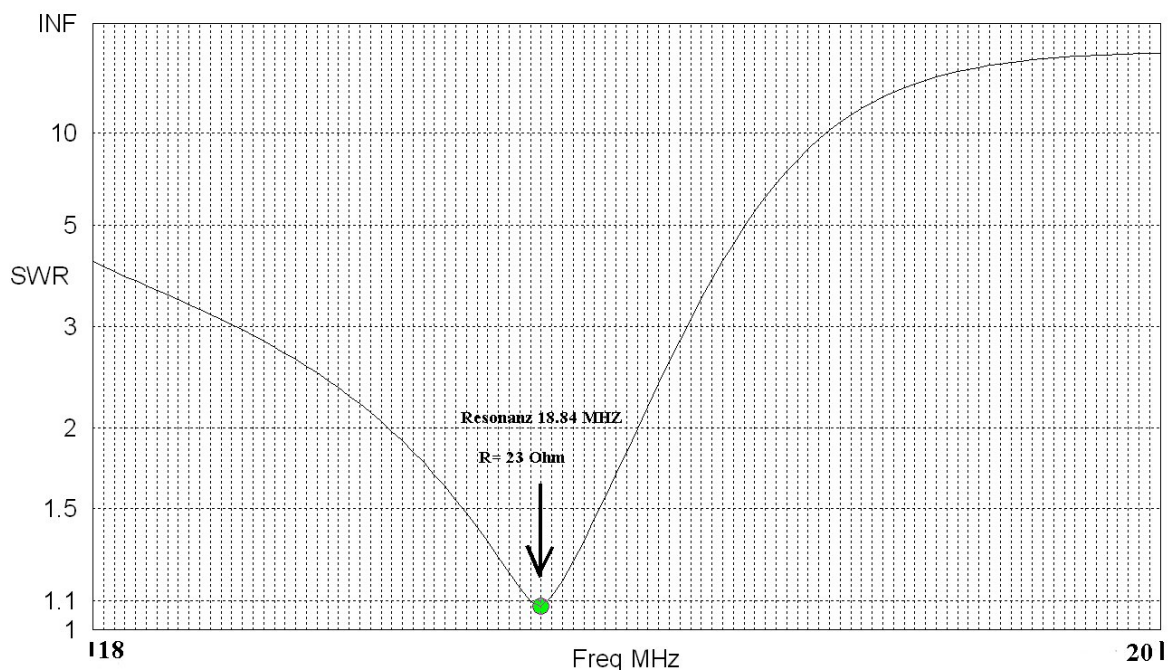


Fig. 10: SWR graph computed with EZNEC, using factory default element lengths for 18 MHz (Tab. 1), normal mode, 22 Ohms feed- point resistance.

The resonance point at 18.84 MHz found with the EZNEC calculation is unexpected and considerably higher than the resonance point found with the measurements. The lowest SWR on the 50 Ohms coax cable showed a value of 1.1 at 18.1 MHz. SteppIR declares that the “factory default element lengths” as well as the element lengths displayed on the controller unit are true physical lengths. The NEC algorithm takes into account the shortening of the element lengths due to the length to diameter ratio but it does not include the dielectric loading caused by the fiberglass poles. Thus the physical element length needed for the actual resonance point is shorter than what NEC (or EZNEC) considers. In consequence, for computer modelling the element lengths as displayed with the steppIR controller unit have to be multiplied by a factor of $18.84/18.1 = 1.04$. In this case, the operating frequency can be the input value for the computer model, (f.i. 18.1 MHz). The factor of 1.04 can be used with sufficient accuracy for the bands from 14 MHz to 28 MHz. More practical, however, is to accept the lengths dimensions as given by the steppIR controller unit, together with the resonance frequency shown in the computed SWR curve (as in fig. 10).

A comparison of a radiation pattern computed with EZNEC and a pattern obtained from measurements is shown in fig. 11. The pattern obtained from the measurements equates to fig. 8b. The input file for the EZNEC computation used the corresponding data with a resonant frequency of 18.84 MHz. The agreement with the patterns is quite satisfactory. SteppIR claims for 18 MHz and “normal mode” a F/B Ratio of 44 dB and a F/R Ratio of 25 dB. Fig. 11 shows for the measured data 25 dB both for the F/B- and F/R Ratio. It is now attractive to apply a modification of the element lengths to find out whether these results might be improved. For the antenna of DL9CI, an optimum result was obtained shortening the reflector by 4 inch and remaining the lengths of the director and the driven element. Fig. 12 shows the result. The F/B Ratio is now 35 dB, the F/R Ratio 28 dB. For comparison, fig. 12 in addition depicts an EZNEC computation using the corresponding input data.

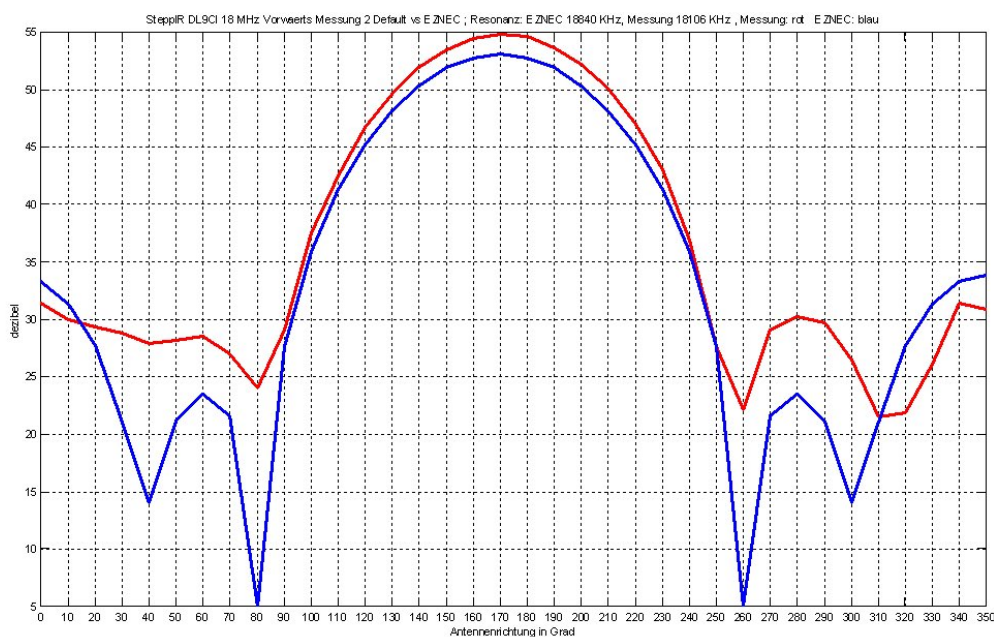


Fig. 11: Comparison of EZNEC computation (blue graph) and measurement data (red curve). Antenna DL9CI, 18 MHz, normal mode, default antenna dimensions.

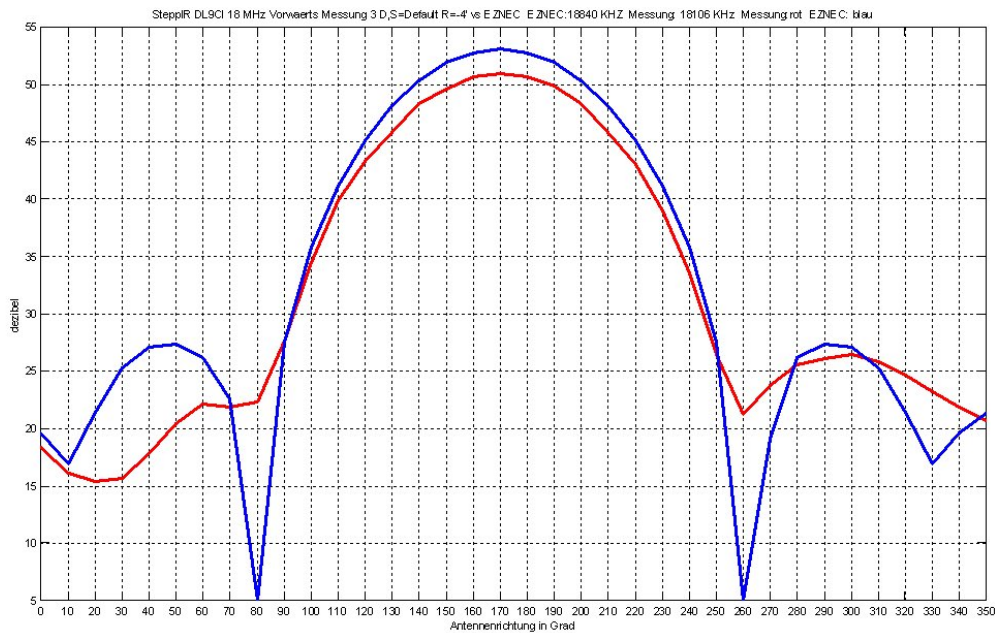


Fig. 12: Comparison of EZNEC computation (blue graph) and measurement data (red curve). Antenna DL9CI, 18 MHz, normal mode, antenna dimensions modified for optimum F/B- and F/R Ratio.

Following fig. 8a, the antenna at DJ3AA with default element lengths shows a F/B Ratio between 15 dB and 20 dB (the minimum is close to the limit stop of the antenna rotator), the F/R Ratio is about 15 dB. These values could be significantly improved after modifying the elements to the following lengths:

Director = 291.3 inch Driven Element = 302.2 inch Reflector = 314.4 inch

The F/B Ratio increased to 30 dB, the F/R Ratio to 25 dB (fig. 13)

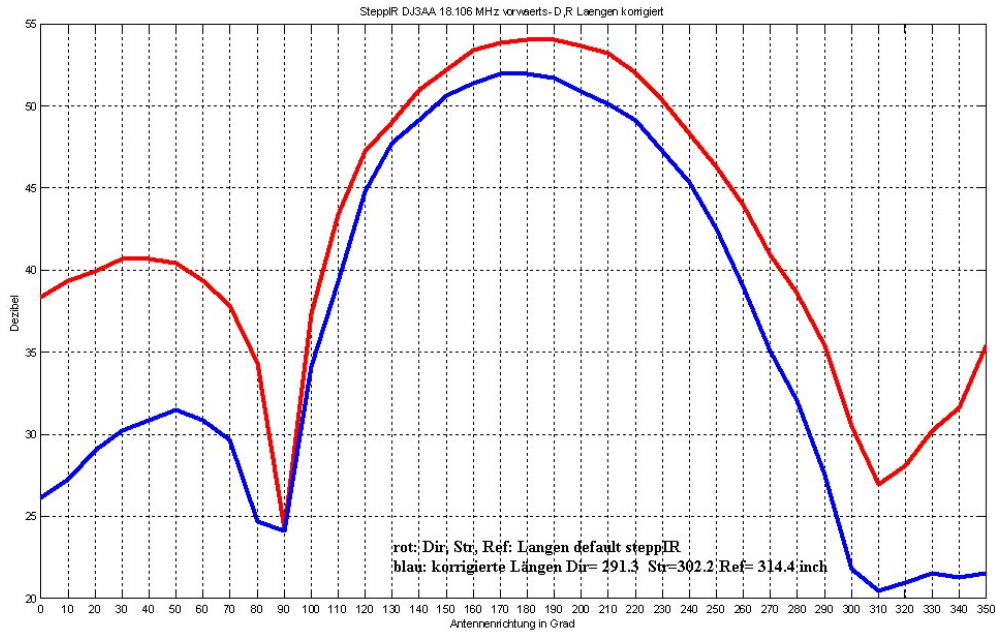


Fig. 13: Radiation pattern of antenna DJ3AA, normal mode. Element lengths factory default: red curve, modified element lengths: blue curve.

Fig. 12 and fig. 13, as well as fig. 19, show a certain unbalance with the side lobes on the rear side of the radiation pattern. Repeated measurements indicated that the unbalance is not caused by measurement errors. Side reflections from nearby obstacles or hills can also be excluded. A likely origin might be found in an (even small) current unbalance at the feeding point of the driven element, f.i. caused by mantle waves on the coax cable. The result is a “monopole radiation” from one branch of the driven element. The superimposed energy on the radiation field is much more noticeable in that part of the radiation pattern where the energy level is low, i.e. in the minor lobes on the back side. As most of the radiated energy is concentrated in the major lobe (fig. 14), its symmetry is very little affected (fig. 17). Fig. 15 gives an illustration assuming a 1% current unbalance at the feeding point.

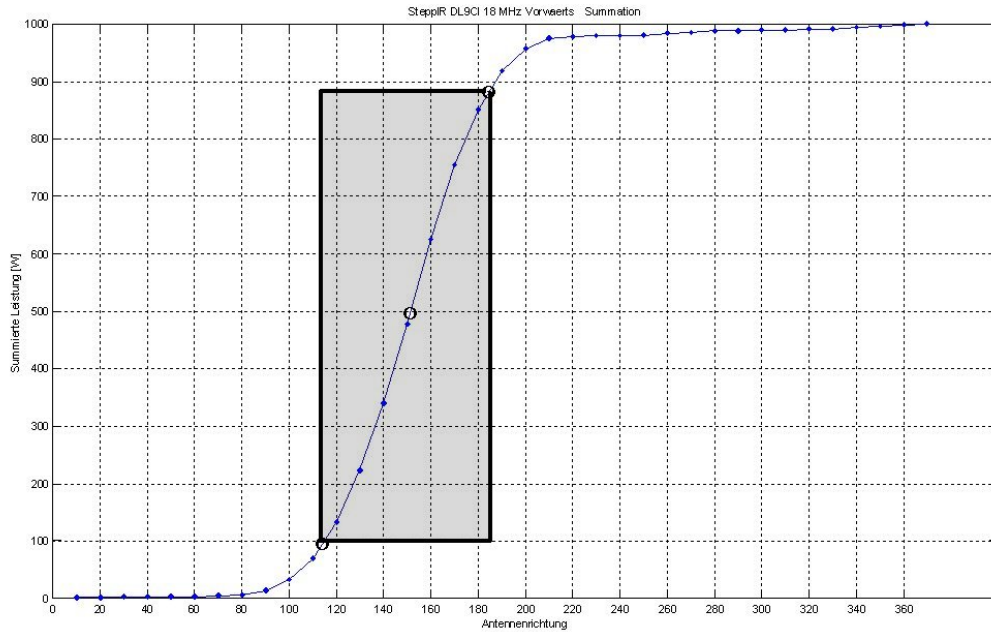


Fig. 14: Summation of the radiated power over the azimuth angle (DL9CI, 18 MHz, normal mode). The shaded area covers the half power bandwidth and contains 80 % of the total radiated power.

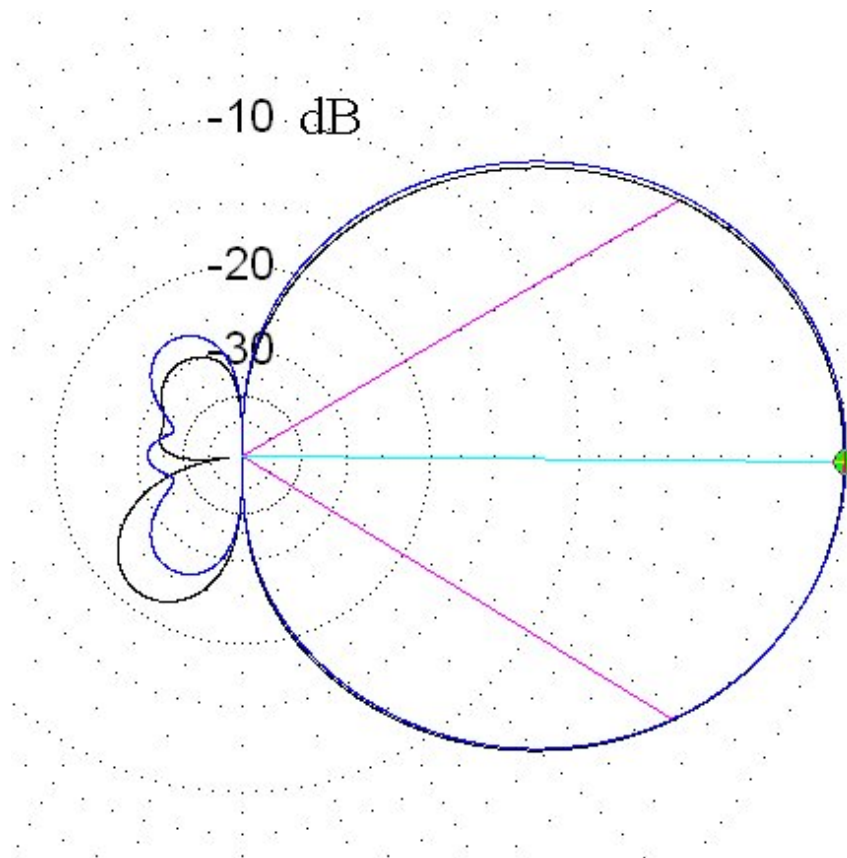


Fig. 15: EZNEC computation of the radiation pattern (polar coordinates) with input data following fig. 13 (Blue curve). The black curve was computed assuming a current unbalance of 1% at the feed point of the driven element. The current unbalance leads to a remarkable distortion in the rear side of the radiation pattern. The main lobe is practically not affected.

Antenna Gain

Gain and directivity are closely related. The antenna gain was estimated via the half power (or minus 3 dB) bandwidth points of the main lobe..

DL6WU (ref. in DL1BU, CQ DL 3/81)) investigated in a comprehensive experimental and theoretically supported study various relationships between the 3 dB power bandwidth of the major lobe and the antenna gain. The given diagrams include correction factors to account for the suppression of the the side- and back-lobes. This correction was done following the data from fig. 14. The result is shown in the graph in fig. 16. Overlaid in the diagram are data points referring to different antennas. The DL6WU graph was extended beyond 70 degrees by the authors using data from literature.

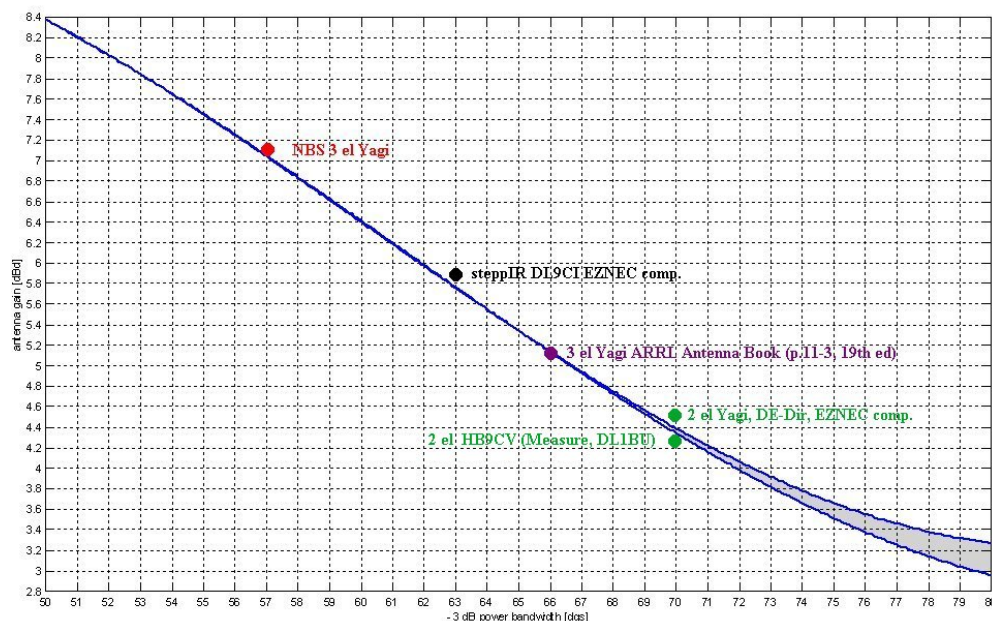


Fig. 16: Variation of antenna gain [dBd] with half power bandwidth, horizontal E-Field. Graph after DL6WU (following a correction factor for the DL9CI antenna), figure overlaid with data points for various antennas. The measured steppIR half power point with the addition of a corresponding EZNEC computation for the DL9CI antenna fits well to the DL6WU graph.

Fig. 17 illustrates a comparison of the measured main lobe from the optimised antenna with DL9CI (fig. 12) and the graph from an EZNEC computation with the corresponding antenna dimensions. The agreement is very convincing. A half power bandwidth of 63 degrees can be read from fig. 17. Following fig. 16, the antenna gain would be close to 6 dBd. For 18 MHz and normal mode operation, steppIR specifies a calculated gain of 6.2 dBd and a measured gain of 5.5 dBd. However, steppIR says nothing about the methods they used to obtain the given values. The gain estimation using the half power bandwidth does not contain electrical loss in the antenna system. Thus the gain estimation with the antenna of DL9CI seems to be agreeable with the values given from steppIR.

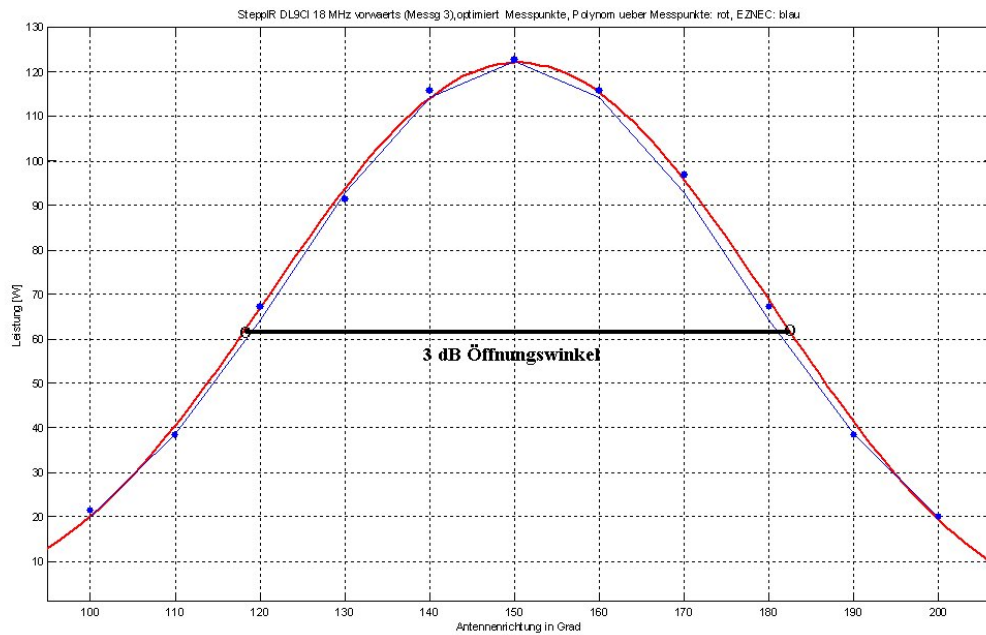


Fig. 17: Comparison of the main lobe of the optimised antenna with DL9CI: blue measuring points with overlaid polynomial fit (red graph), and EZNEC computation following the corresponding antenna dimensions (blue graph). The agreement is very remarkable. Half power band width is close to 63 degrees

Contrary to the antenna of DL9CI, the forward lobe with the antenna of DJ3AA shows a wide half power band width of close to 80 degrees (fig. 18). This bandwidth is all the more not explainable, as the F/R- and F/B Ratio is comparable to the antenna of DL9CI. Following fig. 16, the 80 degrees bandwidth decreases the antenna gain to not much more than 3 dBd. The wide bandwidth in the main lobe is not confined to 18 MHz. Fig. 19 shows a comparison of the radiation patterns of the antennas of DL9CI and DJ3AA for 14 MHz. In addition, fig. 19 contains the pattern of the KLM 4 element Yagi of DJ3VW (Distance DJ3VW-DL3AO 2.28 km, no obstacles). Further studies are necessary for the explanation of the apparent anomaly with the steppiR antenna of DJ3AA.

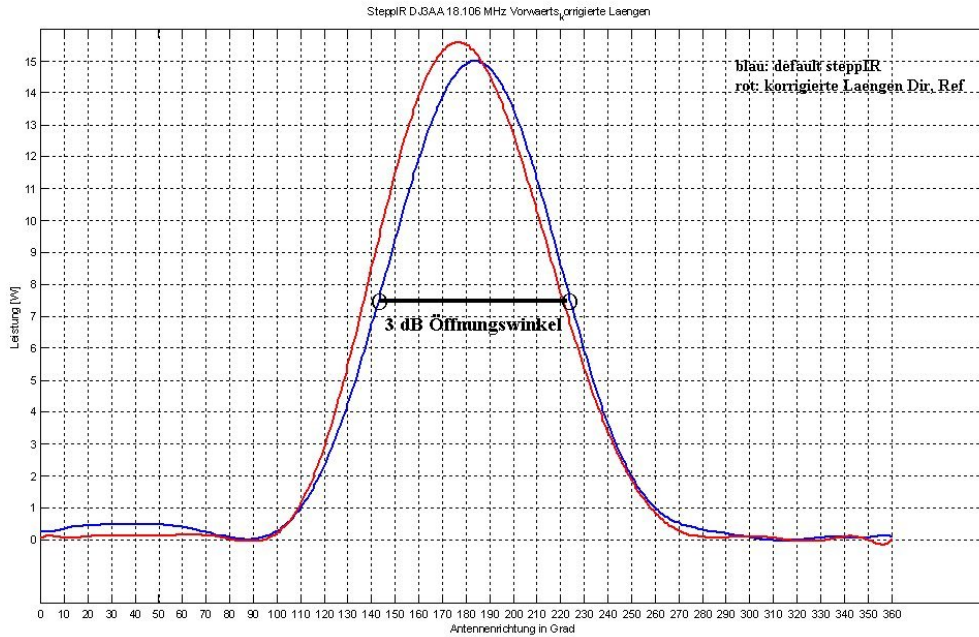


Fig. 18: Main lobe of antenna DJ3AA, 18 MHz, normal mode. Default dimensions: Blue curve, optimised dimensions: Red curve. Optimising the antenna dimensions had no effect on the half power bandwidth.

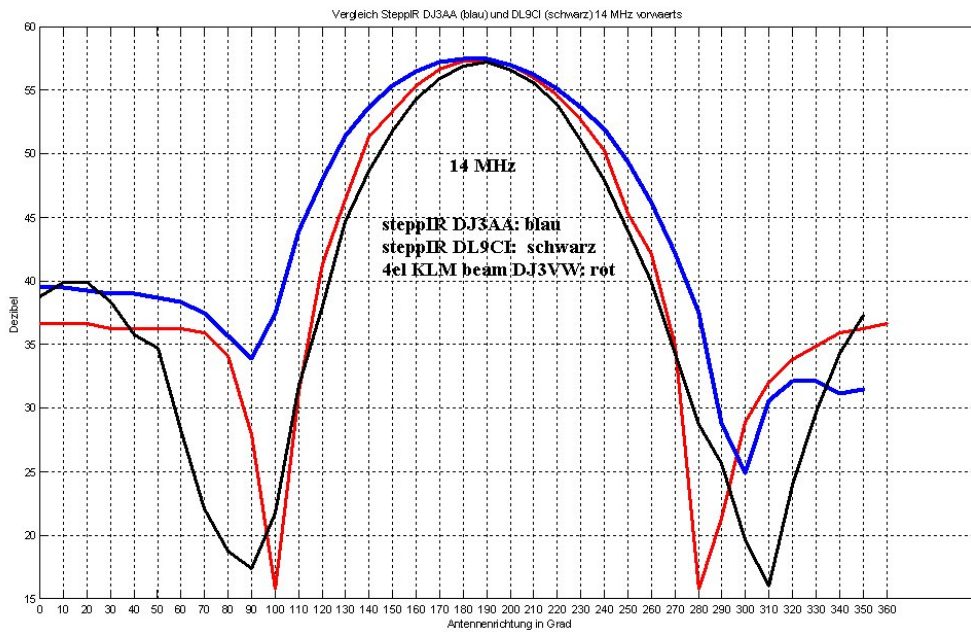


Fig. 19: Comparison of the radiation patterns for the antennas of DL9CI (black curve) and DJ3AA (blue curve), 14 MHz, normal mode. The fig. shows in addition the radiation from a 4 element KLM Yagi with DJ3VW (red curve).

Acknowledgement.

Wolfgang Hummel, DJ3VW, provided the noise generator and the attenuator.

